# LDV MEASUREMENTS IN A RECTANGULAR SURFACE JET

**Soheil Gholamreza-Kashi**
Department of Civil and Environmental Engineering
University of Western Ontario
London, Ontario, N6A 5B9, Canada
sgholamr@uwo.ca

**Robert J. Martinuzzi**
Department of Mechanical and Manufacturing Engineering
University of Calgary
Calgary, Alberta, T2N 1N4, Canada
rmartinu@ucalgary.ca

**Raouf E. Baddour**
Department of Civil and Environmental Engineering
University of Western Ontario,
London, Ontario, N6A 5B9, Canada
rbaddour@eng.uwo.ca

## ABSTRACT

The flow field for a non-buoyant rectangular surface jet was studied using Laser Induced Fluorescence and Laser Doppler Velocimetry. Laminar and turbulent regimes were considered. After an initial development, the jet reached a self-similar state. While the horizontal profiles of the stream-wise velocity were similar to those observed in free jets, the vertical distributions were distinctly flat. In agreement with previous studies, the development of a thin surface current, whose lateral growth rate was twice the lateral growth rate of the bulk of the jet, was observed. The surface current formed as a result of turbulence anisotropy imposed by the surface boundary. Unlike the bulk of the jet below the surface, surface current entrained little ambient fluid and mostly spread radially.

## INTRODUCTION

Surface jets are relevant to many engineering applications, ranging from remote sensing of the wake of a ship to anticipating the environmental impacts of the discharge of pollutants into rivers, lakes, and oceans. It is important to understand the structure of the jet because mixing and transport of scalars, such as temperature, oxygen, and chemical species are governed by the jet turbulence characteristics.

Surface jets differ from free jets and wall jets in many critical aspects that control transport and diffusion. In a free jet, the mixing lengths are not restricted and remain large at the jet centre-line. In a surface jet however, vertical turbulent fluctuations diminish at the surface and mixing lengths decrease accordingly. Turbulent intensities near a surface boundary are smaller compared turbulent intensities near a wall boundary, since wall shear stresses are not present. Surface tension may also modify the lateral spreading of a jet at the surface (Anthony and Willmarth, 1992). Furthermore, it can be argued that rectangular jets are different from circular jets. Stream-wise rotating structures, generated at the corners of the rectangular jet-exit, persist downstream (Quinn, 1992) and interact with the free surface.

Little experimentation has been conducted for non-buoyant rectangular surface jets. Vanvari and Chu (1974) studied plane surface jets. They showed the self-similarity of the velocity profiles, but their results appeared to be affected by the limited depth of their channel. They reported a break down in the linear growth of the jet as early as $x/h_0 = 25$. Rajaratnam and Humphries (1984) measured the mean stream-wise component of the velocity for plane, circular and rectangular surface jets. The results also suggested that a self-similarity region for the velocity profiles exists. However, the conclusions drawn from this work were limited since the scatter in their data was significant, possibly due to the intrusive measurement devices they used. Swean et al. (1989) investigated the effects of confinement on the development of plane surface jets. They showed that the jet remained unaffected by the channel bed up to a downstream distance equal to the depth of the channel.

Anthony and Willmarth (1992) conducted LDV measurements for a circular jet issuing beneath a free surface at a distance of twice the jet-exit diameter from the free surface. They discovered that downstream, where the jet reached the free surface, a thin layer of flow formed at the surface, which spread faster than the jet fluid below. They called this thin layer of flow "surface current". Walker et al. (1995) studied the effects of Reynolds number and Froude number on the turbulence structure of circular jets issuing beneath a free surface at a distance of twice the jet-exit diameter from the free surface, using LDV. They observed at the free surface, that turbulence energy was transferred from diminishing vertical velocity fluctuations to tangential velocity fluctuations through tangential velocity-vorticity correlation. Walker (1997) further investigated the origin of the surface current in turbulent free-surface flows and concluded that it can be rep-

resented equivalently by either the Reynolds stress anisotropy or the correlation of tangential velocity and vorticity near the free surface, both of which originate from the surface boundary condition that the vertical velocity must vanish. Martinuzzi et al. (1998) examined the turbulence structure of plane, two-dimensional surface jets in a weak ambient flow for different initial exit conditions using LDV. These results showed that the linear growth region is rapidly established and the jet reached self-similarity. It was observed that the stream-wise velocity profiles in this self-similar region were much flatter than those observed for free jets.

The fundamental motivation for this study is to investigate and document the self-similar development of both the mean and turbulence quantities for a rectangular surface jet. In contrast to earlier works, where the jet was initially submerged, the present jet develops at the surface over a shorter distance, allowing investigation of the development of both the surface current and the submerged portion of the jet.

## EXPERIMENT

The flow apparatus consisted of three sections: (1) 1.30 m long, 0.80 m wide, and 0.40 m deep testing section made of glass; (2) 0.50 m long, 1.50 m wide, and 1.00 m deep stilling tank made of steel; (3) 0.25 m long, 0.25 m wide, and 0.40 m deep inlet chamber made of steel. To create a uniform velocity profile at the jet-exit, the inlet chamber was constructed as a convergent nozzle with vertical and horizontal curvatures. Water flowed from a constant head-tank into the inlet chamber and was released at the free surface of the testing section. The water overflowed from the weirs installed at the surface of the stilling tank and was pumped back into the constant-head tank. Flow was circulated to keep the fluid properties and the seeding uniform throughout the apparatus. The stilling tank was incorporated to minimize the effects of confinement.

The flow conditions at the jet-exit, namely width, $b_0$, depth, $h_0$, initial velocity, $U_0$, aspect ratio, $h_0/b_0$, and Reynolds and Froude numbers for different experiments are summarized in Table 1. Reynolds numbers were calculated based on the initial jet hydraulic diameter, and Froude numbers based on the initial depth of the jet. In all experiments, the flow at the jet-exit was subcritical.

The jet flow was visualized using a Laser Induced Fluorescence (LIF) visualization technique. The 488 nm (blue) line of a 4 W Argon-Ion laser was used to excite the fluorescence dye, which reemitted at 520 nm. Dye was added to the jet tank at a constant rate. A cylindrical lens was applied to produce an approximately 4 mm thick laser sheet, which was oriented either horizontally, parallel to the surface, or vertically, parallel to the jet axis or normal to it. Images formed from fluorescence emission were recorded digitally at a rate of 60 frames per second. A 500 nm high-pass light filter was used to suppress the excitation blue light and allow only the fluorescent light to be recorded, thus reducing background light noise.

The velocity measurements were conducted using a TSI two-component Laser Doppler Velocimetry system in backscatter mode. The transmitting lens had a focal length (in air) of 350 mm, resulting in a measuring volume diameter and length of 0.046 mm and 1.2 mm, respectively. Data were collected using single measurement per burst (SMB) mode. A three-axis motor driven traversing unit were used to move the LDV probe in all three directions, with a relative position accuracy (precession) of 0.015 mm per 100 mm of travel and a minimum displacement of 0.0025 mm per step. Vertical velocity profiles were measured in the jet plane of symmetry, by positioning the probe at the side of the tank. Horizontal velocity profiles were measured at approximately 1 mm below the free surface, and at the jet vertical half-width, by positioning the probe below the tank. The flow was seeded using Silicon Carbide particles with an average diameter of 2 $\mu$m and a density of 3.2 g/cc. These particles were added to increase the effective data rate by roughly a factor of 10. Velocity profiles measured with naturally suspended particles (i.e. no seeding) were used as comparison and were found to agree within experimental uncertainty. Measurements were conducted at seven downstream locations: $x/h_0 = 4$, 8, 12, 16, 24, 32, and 40.

The estimated maximum measurement uncertainty of the velocity was calculated to be $0.0086\,U_0$ with a 95 percent confidence level as proposed by Abernathy et al. (1985). The uncertainty for the jet momentum was then calculated according to Doeblin (1975) to be $0.023\,U_0^2\,b_0\,h_0$.

## RESULTS AND DISCUSSIONS

Figures 1 and 2 show cross-sectional images of jet I and II, respectively, in a vertical plane positioned at $x/h_0 = 20$ normal to the jet axis. The free surface in these images is at $z/h_0 = 0$. What is seen above this level is only a reflection. Time sequences of the image shown in Fig. 2 indicated that stream-wise vortices entrained fluid from below the jet upward along the centre. The fluid was deflected at the surface and ejected laterally giving rise to a thin surface layer. The thin surface layer spread laterally at a higher rate than the jet fluid below the surface. Ejection of the fluid occurred alternately to the right and the left of the jet centre-plane. However, the visualisation results and the velocity time series suggested that this cyclical alternation was non-periodic in nature. Anthony and Willmarth (1992) and Walker et al. (1995) have reported a similar phenomenon when submerged round jets interacttd with the free surface. As Walker (1997) explained, the lateral acceleration of this surface current was due to the significant imbalance between vertical and lateral Reynolds normal stresses, which is caused by the turbulence anisotropy created near the free surface. This mechanism does not exist in the laminar surface jet flow, and hence the surface current is not observed as evidenced by the visualisation of Fig. 1.

Furthermore, the authors believe that stream-wise vortices generated at the bottom corners of the rectangular jet exit can also contribute to this lateral spreading. In Fig. 1, the presence of these vortices in the lower corners can be inferred. In the case of the laminar jet, there is little transverse and vertical mixing, so that the effect of the corner vortices remains local.

Fig. 3 shows vertical profiles of mean stream-wise velocity of jets IV and V, measured in the plane of symmetry. Velocity is normalized by the local maximum velocity, $U_{max}$, which occurs at the surface. Location is normalized by $L_z$, the local jet vertical half-width, at which the velocity is equal to the half the local maximum velocity, $U_{max}$. Solid symbols represent jet IV ($Re = 4420$), and open symbols represent jet V ($Re = 8850$). Similar to a plane surface jet (Martinuzzi et al., 1998), three distinct regions can be identified: (i) a potential core at $x/h_0 = 4$, where the jet is characterized by an almost uniform profile (Fig. 3.a); (ii) a development region between $x/h_0 = 4$

Table 1: Flow parameters for different experiments

| Experiment | Jet | $b_0$ (m) | $h_0$ (m) | $h_0/b_0$ | $U_0$ (m/s) | Re | Fr |
|---|---|---|---|---|---|---|---|
| **LIF** | **I** | 0.056 | 0.028 | 0.50 | 0.024 | 1340 | 0.05 |
| | **II** | 0.056 | 0.028 | 0.50 | 0.181 | 10,100 | 0.35 |
| | **III** | 0.056 | 0.028 | 0.50 | 0.402 | 22,400 | 0.77 |
| **LDV** | **IV** | 0.025 | 0.013 | 0.52 | 0.175 | 4420 | 0.49 |
| | **V** | 0.025 | 0.013 | 0.52 | 0.349 | 8850 | 0.98 |

and $x/h_0 = 16$, where the profiles can be approximated by a Gaussian distribution (Fig. 3.a); and (iii) a fully-developed region beyond $x/h_0 = 16$, where the profiles are almost linear (Fig. 3.b). All profiles collapse in the fully-developed region, indicating that the jet reaches a self-similar state in this region. The flat stream-wise velocity profiles in the fully developed region were also observed by Martinuzzi et al. (1998) for plane surface jets.

Figure 4.b shows horizontal profiles of mean stream-wise velocity of jet V in the fully-developed region, measured below the surface at the location of jet vertical half-widths, $L_z$. Velocity is normalized by the local maximum velocity, $U_{max}/2$, and location is normalized by the local jet horizontal half-width, $L_y$. All profiles collapse fairly well. The shape of these profiles approaches a Gaussian distribution, similar to those observed for free jets.

Horizontal profiles of mean stream-wise velocity of jets IV and V, measured at the surface, are shown in Fig. 4.a. Velocity is normalized by the local maximum velocity, $U_{max}$, and location is normalized by the local jet horizontal half-width at the surface, $L_{ys}$. Symmetry of velocity profiles about x-axis was verified for selected profiles. In the fully-developed region all profiles collapse on a single curve. It is interesting to note that unlike the deeper horizontal profiles (Fig. 4.b), these profiles do not have a Gaussian distribution. The velocities do not go to zero at the tail of the profiles, creating a pedestal. A very similar pedestal was also observed in the horizontal velocity profiles of Anthony and Willmarth (1992), Walker et al. (1995), and Walker (1997). It is unlikely that this pedestal is due to confinement effect, since the present and earlier jets differ significantly in physical dimensions of the tank relative to the jet as well as the momentum and mass fluxes. Furthermore, the pedestal only appears in the surface layer, and is not observed in the deeper horizontal profiles (Fig. 4.b) or in vertical profiles (Fig. 3). The authors believe that this pedestal is due to the fact that the surface current entrains little ambient fluid and mostly spreads radially.

Figure 5 shows the horizontal profiles of mean lateral velocity, V, of the jets IV and V in the fully-developed region, measured at the surface (Fig. 5.a) and below the surface at $z = L_z$ (Fig. 5.b). Velocity is normalized by the local maximum velocity, $U_{max}$, in Fig. 5.a, and $U_{max}/2$, in Fig. 5.b. Location is normalized by the local jet horizontal half-width at the surface, $L_{ys}$, in Fig. 5.a, and the local jet horizontal half-width, $L_y$, in Fig. 5.b. While the velocity profiles below the surface collapse fairly well (Fig. 5.b), at the surface self-similarity is reached more slowly (Fig. 5.a). This is consistent with Walker et al. (1995), who suggested that the surface current requires some stream-wise distance to develop. The lateral velocity at the surface increases up to a peak at $y = L_{ys}$ and then decreases gradually, but remains positive at all time (Fig. 5.a). This outflow gives rise to the pedestal at the tail of the stream-wise velocity profiles in Fig. 4.a. The maximum lateral velocity at the surface is about 20% of the maximum stream-wise velocity, which is roughly twice the maximum lateral velocity below the surface, and consistent with the observed increase in the lateral growth rate at the surface. Lateral velocity below the surface also increases up to a peak at $y = L_y$ and then decrease gradually, but it becomes negative at about $y = 2\,L_y$ (Fig. 5.b), indicating that while the jet flow below the surface entrains ambient fluid, the surface current mostly ejects jet fluid outward, as observed by flow visualizations.

Horizontal profiles of Reynolds shear stress of the jets IV and V measured at the surface and the jet V measured below the surface at $z = L_z$, are shown in Fig. 6.a and 6.b respectively. The maximum shear stress at the surface (Fig. 6.a) is about one third the maximum shear stress below the surface (Fig. 6.b), indicating that turbulent mixing in the surface current is small comparing to that in the jet flow below, and the surface flow is mostly spreading radially outwards, as explained earlier and seen in visualizations.

Figure 7.a shows the turbulence kinetic energy distribution, k, in the jet plane of symmetry. k is defined as sum of the Reynolds normal stresses, divided by two, or $\overline{u_i u_i}/2$. Vertical profiles of Reynolds normal stresses in the jet plane of symmetry, normalized by 2k, are shown in Fig. 7.b to Fig. 7.d. For $z < 0.5\,L_z$, while vertical component of the Reynolds normal stress, $\overline{w^2}$, diminishes (Fig. 7.d), tangential components, $\overline{u^2}$ (Fig. 7.b) and $\overline{v^2}$ (Fig. 7.c) increase. This shows that close to the surface, turbulence energy has to be redistributed to compensate for diminishing vertical velocity fluctuation. As mentioned in previous studies, the turbulence anisotropy created by the energy redistribution close to the surface is closely connected to the development of the surface current.

## CONCLUSIONS

LIF flow visualizations and LDV measurements were carried out in the plane of symmetry and in horizontal planes below and at the surface of a non-buoyant rectangular surface jet. Laminar and turbulent regimes over a range of Reynolds numbers were investigated. Flow visualizations showed a thin surface current, which spread laterally faster than the bulk of the jet fluid below. The existence of a surface layer was previously reported when submerged circular jets interacted with the free surface. Similar to those jets, the turbulence anisotropy close to the surface, caused by redistribution of turbulence energy from vertical to tangential velocity fluctuation, resulted in the development of the surface current. Measurements showed that the lateral growth rate of the surface current was twice the lateral growth rate of the bulk of

the jet.

The jet reached a self-similar state after an initial development. The vertical velocity profiles along the plane of symmetry were much flatter than those observed in free jets, but do resemble those for plane surface jets. Unlike the horizontal profiles below the surface, which have a Gaussian distribution similar to those for classical free jet solutions, velocity profiles in the surface current have a distribution that reflects its radial spreading nature. Turbulence mixing in the surface current was much smaller than that in the bulk of the jet below.

## REFERENCES


Abernathy, R. B., Benedict, P. R., and Dowell, R. B., 1985, "ASME measurement uncertainty," *ASME Journal of Fluid Engineering*, Vol. 107, pp. 161-164.

Anthony, D. G., and Willmarth, W. W., 1992, "Turbulence measurements in a round jet beneath a free surface," *Journal of Fluid Mechanics*, Vol. 243, pp. 699-720.

Deoblin, O. E., 1975, Measurement Systems, Applications and Design, McGraw-Hill, New York.

Martinuzzi, R., Zaghloul, A. M., Al-Qaraguli, W., and Baddour, R. E., 1998, "Turbulence structure of plane surface-jets in a weak coflowing stream for different initial wake conditions," *ASME Journal of Fluid Engineering*, Vol. 120, pp. 76-82.

Quinn, W. R., 1992, "Streamwise evolution of a square jet cross section," *AIAA Journal*, Vol. 30(12), pp. 2852-2857.

Rajaratnam, N., and Humphries, J. A., 1984, "Turbulent non-buoyant surface jets," *Journal of Hydraulic Research*, Vol. 22(2), pp. 103-115.

Swean Jr., T. F., Ramberg, S. E., Plesniak, M. W., and Stewart, M. B., 1989, "Turbulent surface jet in channel of limited depth," *ASCE Journal of Hydraulic Engineering*, Vol. 115(12), pp. 1587-1606.

Vanvari, M. R., and Chu, V. H., 1974, "Two-dimensional turbulent surface jets of low Richardson number," Technical Report 74-2[FML], Fluid Mechanics Laboratory, Department of Civil Engineering and Applied Mechanics, McGill University, Montreal, Canada.

Walker, D. T., Chen, C.-Y., and Willmarth, W. W., 1995, "Turbulent structure in free-surface jet flows," *Journal of Fluid Mechanics*, Vol. 291, pp. 223-261.

Walker, D. T., 1997, "On the origin of the 'surface current' in turbulent free-surface flows," *Journal of Fluid Mechanics*, Vol. 339, pp. 275-285.


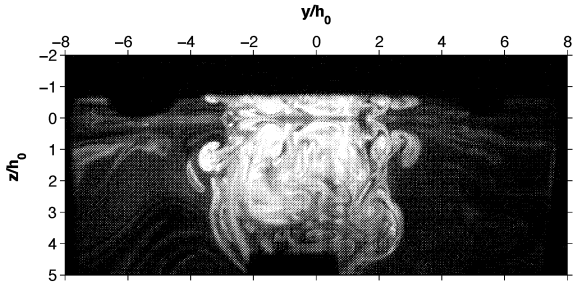


Figure 1: Visualization of jet I
in a cross-sectional plane at $x/h_0 = 20$

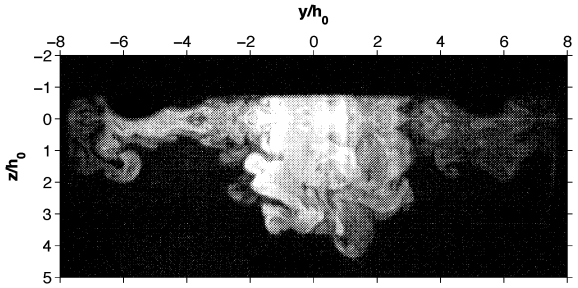


Figure 2: Visualization of jet II
in a cross-sectional plane at $x/h_0 = 20$

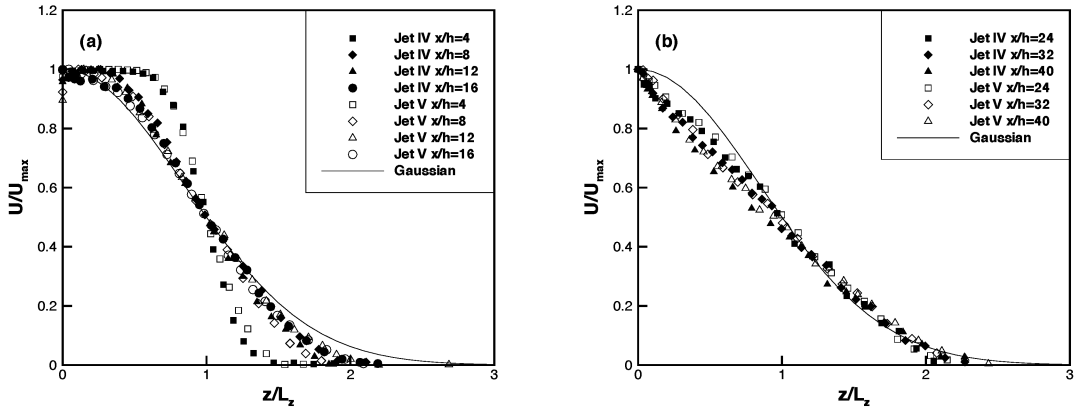


Figure 3: Vertical profiles of mean stream-wise velocity in the jet plane of symmetry in the development region (a) and the fully-developed region (b)

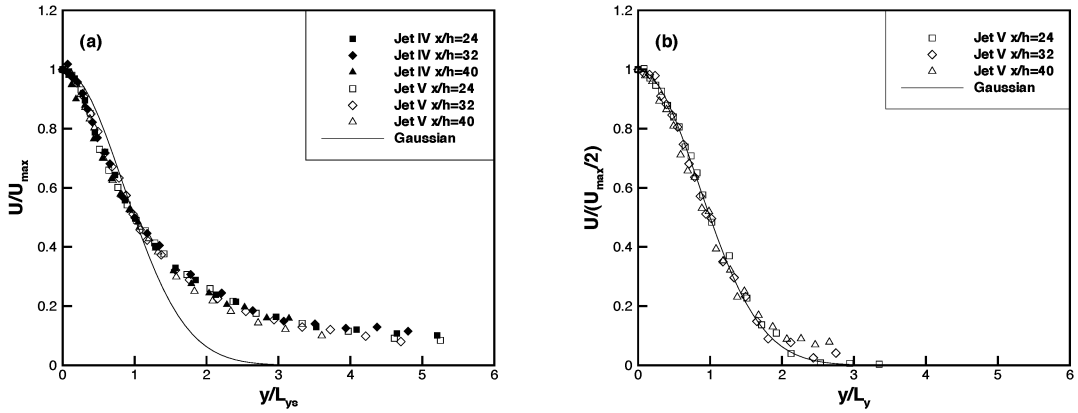


Figure 4: Horizontal profiles of stream-wise velocity at the surface (a) and below the surface at $z = L_z$ (b)

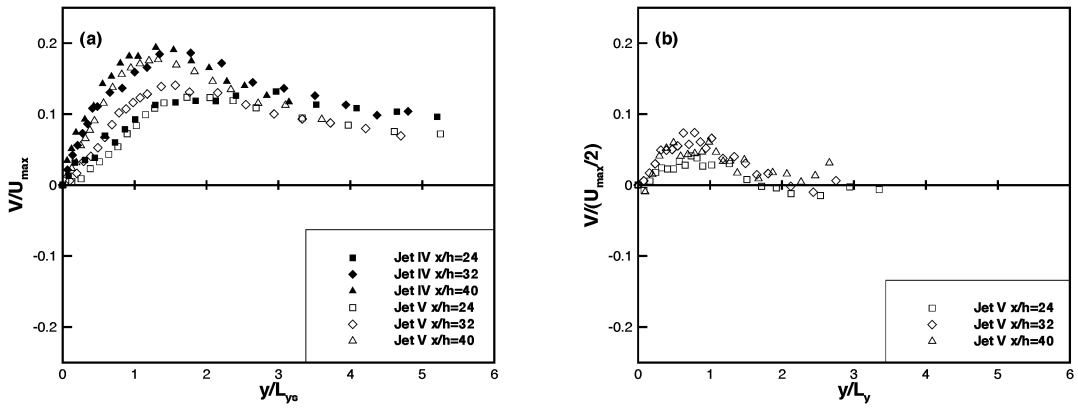


Figure 5: Horizontal profiles of mean lateral velocity at the surface (a) and below the surface at $z = L_z$ (b)

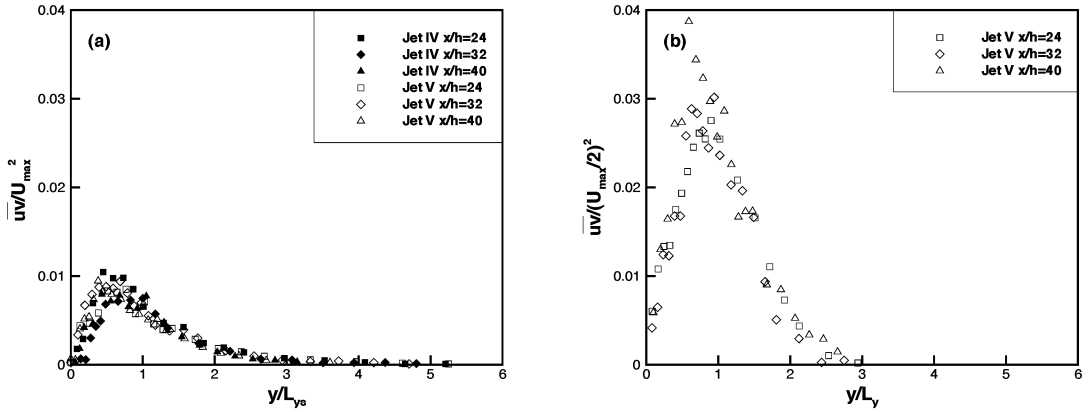


Figure 6: Horizontal profiles of Reynolds shear stress $\overline{uv}$ at the surface (a) and below the surface at $z = L_z$ (b)

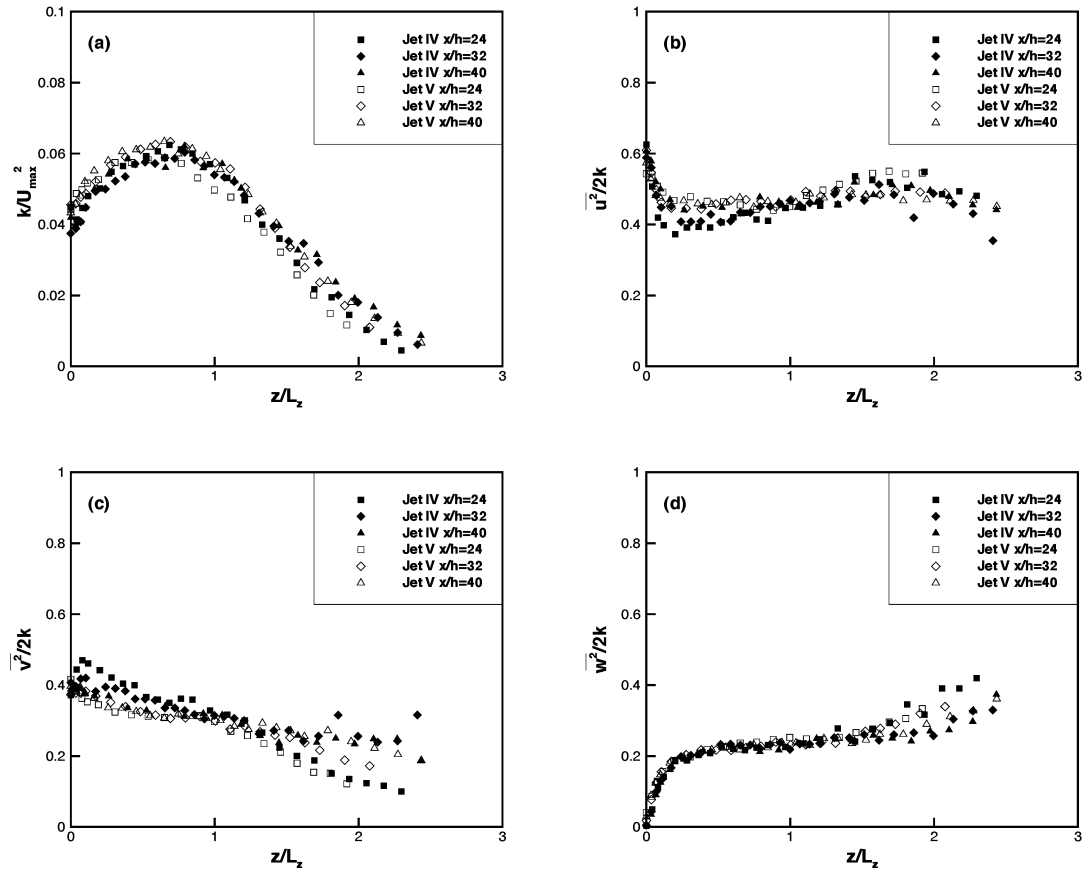


Figure 7: Vertical profiles of turbulence kinetic energy (a) and
stream-wise (b), lateral (c), and vertical (d) components of Reynolds normal stress in the jet plane of symmetry